



A quantitative chloride channel conductance assay for efficacy testing of AAV.BEST1

DOI:
[10.1089/hgtb.2018.267](https://doi.org/10.1089/hgtb.2018.267)

Document Version
Accepted author manuscript

[Link to publication record in Manchester Research Explorer](#)

Citation for published version (APA):

Wood, S., McClements, M. E., Martinez-Fernandez de la Camara, C., Patricio, M. M., Uggenti, C., Sekaran, S., Barnard, A. R., Manson, F., & MacLaren, R. E. (2019). A quantitative chloride channel conductance assay for efficacy testing of AAV.BEST1. *Human Gene Therapy Methods*. <https://doi.org/10.1089/hgtb.2018.267>

Published in:
Human Gene Therapy Methods

Citing this paper

Please note that where the full-text provided on Manchester Research Explorer is the Author Accepted Manuscript or Proof version this may differ from the final Published version. If citing, it is advised that you check and use the publisher's definitive version.

General rights

Copyright and moral rights for the publications made accessible in the Research Explorer are retained by the authors and/or other copyright owners and it is a condition of accessing publications that users recognise and abide by the legal requirements associated with these rights.

Takedown policy

If you believe that this document breaches copyright please refer to the University of Manchester's Takedown Procedures [<http://man.ac.uk/04Y6Bo>] or contact uml.scholarlycommunications@manchester.ac.uk providing relevant details, so we can investigate your claim.



Title: A quantitative chloride channel conductance assay for efficacy testing of AAV.BEST1

Authors: Shaun R Wood¹, Michelle E McClements¹, Cristina Martinez-Fernandez de la Camara¹, Maria I Patrício¹, Carolina Uggenti², Sumathi Sekaran¹, Alun R Barnard¹, Forbes D Manson² and Robert E MacLaren^{1,3,4}.

- 1. Nuffield Laboratory of Ophthalmology, Department of Clinical Neurosciences, University of Oxford, OX3 9DU.**
- 2. Division of Evolution and Genomic Sciences, The University of Manchester, M13 9PT.**
- 3. National Institute for Health Research (NIHR) Oxford Biomedical Research Centre (BRC), Oxford, UK.**
- 4. Oxford Eye Hospital, Oxford University Hospitals NHS Foundation Trust, Oxford, UK.**

Correspondance:

enquires@eye.ox.ac.uk or Forbes.Manson@manchester.ac.uk

Abstract

Mutations in the human *BEST1* gene are responsible for a number of distinct retinal disorders known as ‘bestrophinopathies’, for which there are no current treatments. The protein product, bestrophin-1, is expressed in the retinal pigment epithelium (RPE) where it localises to the basolateral membrane and acts as a Ca²⁺-activated chloride channel. Recent studies have shown successful BEST1-mediated gene transfer to the RPE, indicating human clinical trials of BEST1 gene therapy may be on the horizon. A critical aspect of such trials is the ability to assess the efficacy of vector prior to patient administration. Here, we present an assay that enables the quantitative assessment of AAV-mediated BEST1 chloride conductance as a measure of vector efficacy.

Expression of BEST1 following transduction of HEK293 cells with AAV.BEST1 vectors was confirmed by liquid chromatography, western blot and immunocytochemistry. Whole-cell patch-clamp showed increased chloride conductance in BEST1-transduced cells compared to sham-transduced and untransduced controls. Exogenous chloride current correlated to BEST1 expression level, with an enhanced AAV.BEST1.WPRE vector providing higher expression levels of BEST1 and increased in chloride conductance.

This study presents *in vitro* electrophysical quantification of bestrophin-1 following AAV-mediated gene transfer, providing vital functional data on an AAV gene therapy product which will support a future application for regulatory approval.

Introduction

Autosomal recessive bestrophinopathy (ARB) is one of the inherited retinal dystrophies that constitute the bestrophinopathies, caused by mutations in *BEST1* [1]. Patients with ARB present in the first or second decade of life with an abnormal electrooculogram (EOG) light peak that is characteristic for this group of diseases. The fundus findings include yellowish subretinal deposits, subretinal fluid accumulation, localized retinal detachment and abnormal autofluorescence [2-4]. There are currently no treatments for ARB.

Bestrophin-1 protein is a homo-pentameric integral membrane protein that is primarily expressed in the basolateral membrane of the retinal pigment epithelium (RPE) [5]. Although the physiological role of bestrophin-1 has yet to be determined, several functions have been ascribed to it including acting as a Ca^{2+} -activated Cl^- channel (CaCC) and a volume-regulated anion channel (VRAC) [6-9]. Recent studies have also suggested a role for ATP in Bestrophin-1 regulation [10]. *In vitro* testing of bestrophin-1 mutants, via whole-cell patch-clamp, shows deficiencies in these processes [8, 11]. The X-ray crystal structure of bestrophin-1, together with the cell electrophysiology studies supports the hypothesis that bestrophin-1 functions as an anion channel [12, 13].

Missense mutations in bestrophin-1 lead to a loss of chloride conductance *in vitro* [14]. The clinical results of these mutations are similar to those seen in canine multifocal retinopathy, a naturally occurring model of ARB [15]. However the phenotype is not recapitulated in a mouse knockout model [16].

Recombinant adeno-associated virus (rAAV)-mediated gene therapy has emerged as a viable therapeutic strategy to treat inherited degenerations of the retina. In 2017, Luxturna became the first FDA-approved gene therapy treatment for an inherited retinal dystrophy and other clinical trials for a variety of other IRDs are underway and show promising results in the early phase clinical trials for the autosomal recessive condition Leber Congenital Amaurosis (LCA) and the X-linked recessive condition choroideremia have both produced promising results [17-19]. There are also clinical trials underway for a range of other inherited retinal disorders including X-linked retinitis pigmentosa and MERTK-associated retinitis pigmentosa [20]. ARB is amenable to treatment with rAAV gene

This paper has been peer-reviewed and accepted for publication, but has yet to undergo copyediting and proof correction. The final published version may differ from this proof.

Human Gene Therapy
A quantitative chloride channel conductance assay for efficacy testing of AAV-BEST1 (DOI: 10.1089/hgtb.2018.267)

transfer as the *BEST1* coding sequence is within its ~4.7 kb capacity and the RPE has high tropism for AAV gene transfer [21-23]. Proof-of-principle for rAAV-mediated bestrophin-1 transfer has already been demonstrated in the canine model of ARB [24, 25]. These promising studies indicate a clinical trial using AAV.BEST1 vectors may soon be a possibility, meaning there will be need for a quantitative and validated assay that can assess the efficacy of an AAV.BEST1 vector prior to patient administration. Here we describe a novel potency assay in which the restoration of bestrophin-1 mediated chloride current is achieved following AAV gene transfer.

Methods

Production of plasmid constructs and viral vectors

Human *BEST1* coding sequence (NM_004183) was cloned into a pAAV backbone under the control of the ubiquitous cytomegalovirus early enhancer and chicken β -actin hybrid promoter (CAG), with a downstream polyadenylation signal from the bovine growth hormone (BGH pA). One of the plasmids included the woodchuck hepatitis virus posttranscriptional regulatory element (WPRE) in the transgene cassette, between the hBEST1 coding sequence and the polyadenylation signal. In both plasmids, the transgene cassette is flanked by AAV2 internal terminal repeat (ITR) sequences. The integrity of the plasmid constructs was confirmed by Sanger sequencing and XmaI restriction digest through the ITRs.

Recombinant AAV2/2 vectors were produced by transient polyethylenimine (PEI, Sigma-Aldrich) co-transfection of HEK293T cells seeded in HYPERflasks (Corning) using two plasmids: the AAV2 expression plasmid containing either CAG.BEST1 or CAG.BEST1.WPRE and the commercial helper plasmid pDG (Plasmid Factory) encoding *Rep* and *Cap* genes of AAV2 and an adenoviral helper sequence. Viral vectors were purified using iodixanol gradient ultracentrifugation, and concentrated by buffer exchange in Amicon 100K filters (Millipore). To determine rAAV titer, samples were treated with DNaseI for 30 minutes at room temperature, and capsids denatured at 95 °C for 10 minutes. The genome particles per milliliter were analysed by quantitative PCR (qPCR) using primers to the BGH pA

sequence (Forward primer: 5'-CCAGCCATCTGTTGTTTGCC-3', Reverse primer: 5'-GAAAGGACAGTGGGAGTGGC-3').

Cell Culture

HEK293 and HEK293T cells were maintained in Minimum Essential Medium and Dulbecco's Modified Eagle Medium (both Sigma Aldrich, UK), respectively. All media were supplemented with 10% Fetal Bovine Serum (Life Technologies, UK), 1% L-Glutamine (Sigma Aldrich, UK) and 1% Penicillin/Streptomycin (Sigma Aldrich, UK). Cells were incubated at 37°C with 5% CO₂, and passaged upon reaching ~70% confluency.

Immunoprecipitation and protein sequencing

Plasmid encoding human *BEST1* was transfected into HEK293 cells using LT1 Transfection Reagent (Geneflow). Forty-eight hours later, cells were harvested and cell pellets were subjected to a single freeze-thaw cycle before proceeding with the protein extraction using Radio-Immunoprecipitation Assay (RIPA) buffer with protease inhibitors (cOmplete mini EDTA-free protease inhibitor cocktail tablet, Roche Product Ltd.). Cell pellets were disrupted by sonication and the resultant lysates were centrifuged at 13000 rpm for 15 minutes at 4 °C. The total protein content was quantified in the supernatant using the PierceTM bicinchoninic acid (BCA) Protein Assay Kit (Thermo Scientific) according to manufacturer's instructions.

To immunoprecipitate human bestrophin-1 from transfected cell lysates, 10 µl of mouse monoclonal anti-hBEST1 antibody (ab2182, Abcam) was incubated with 100 µl of Protein G Sepharose[®] (Fast Flow, Sigma-Aldrich) for 2 hours at room temperature. Unbound antibody was removed by centrifugation at 3000 g for 2 minutes. 100 µl of the protein lysate was added to the antibody-protein G mixture and incubated overnight at 4 °C. Immunoprecipitates were washed three times in 0.01M PBS with 0.01% Tween 20. Protein complexes were dissociated from beads by incubation at 90-100°C for 10 minutes in 6x Laemmli buffer containing 1.5% SDS (Bioquote limited, York, UK) and isolated with centrifugation at 5000 g for 5 minutes. Immunoprecipitates were resolved via SDS-PAGE followed by EZBlueTM Coomassie Brilliant Blue G-250 (Sigma-Aldrich) staining. The bestrophin-1 protein band was excised from the blue-stained gel and submitted to the

Advanced Proteomics Facility of the University of Oxford for protein identification. The samples underwent proteolytic digestion with trypsin, and the resulting peptide mixtures were separated by liquid chromatography and analysed by tandem mass spectrometry (LC-MS/MS) using the QExactive03, Dionex and Easy-nLC from Thermo Scientific.

Western blotting

HEK293 cells were harvested 72 hours after AAV transduction and protein was extracted and quantified as described above. Twenty to thirty μg of total protein was denatured in protein loading buffer (National Diagnostics) for 30 minutes at room temperature and then loaded into 10% Tris-glycine gels (Criterion TGX Precast Gels; Bio-Rad Laboratories). Protein bands were resolved at 100 V for 2 hours at room temperature and transferred onto polyvinylidene difluoride (PVDF) membranes (Trans-Blot Turbo Midi PVDF; Bio-Rad) using the Trans-Blot Turbo Transfer Starter System (Bio-Rad) running at 25 V for 7 minutes. PVDF membranes were blocked in 1% bovine serum albumin and incubated in primary antibodies for 1 hour at room temperature. Membranes were then incubated in horseradish peroxidase (HRP)-linked secondary antibodies (see supplementary table 6) for 1 hour at room temperature. Detection was performed using chemiluminescence with Luminata forte ELISA HRP substrate (Millipore). Membranes were imaged with an Odyssey FC imaging system (LI-COR Biosciences) and quantified with Image Studio Lite software, version 5.0.

Patch-Clamp Electrophysiology

HEK293 cells were transduced with rAAV-BEST1 vectors in DMEM with supplements and incubated at 37 °C (with 5% CO₂) for 3 days. An rAAV-GFP vector was used to transduce HEK293 cells as a sham control. Cells were re-seeded onto poly-L-lysine (Sigma Aldrich, Cat#P8920) coated glass coverslips and incubated at 37 °C (with 5% CO₂) for at least 8 hours to allow cells to settle. In experiments designed to compare Cl⁻ conductance in HEK293 cells transduced with rAAV2/2.CAG.BEST1.pA and rAAV2/2.CAG.BEST1.WPRE.pA, cells were bathed in an external recording solution containing: 140 mM NaCl, 2 mM CaCl₂, 1 mM MgCl₂, 10 mM HEPES, 10 mM glucose and 30 mM mannitol (osmolarity was 339 mOsm/kg and pH7.4 with NaOH). In experiments where the reduction of Cl⁻ was required,

140 mM $\text{NaC}_6\text{H}_{11}\text{O}_7$ (sodium gluconate) was used in place of NaCl and osmolarity was adjusted to 339 mOsm/kg using mannitol. Micropipettes were pulled from borosillate glass capillaries (World Precision Instruments) with a Narisage pipette puller. These were back-filled, via a Microfil microfilament (World Precision Instruments), with an internal recording solution containing: 20 mM CsCl, 10 mM EGTA, 7.2 mM CaCl_2 , 2 mM MgCl_2 , 10 mM HEPES, 10 mM glucose, 110 mM CsOH and 110 mM aspartic acid (osmolarity was 317 mOsm/kg and pH7.2 with CsOH). Micropipettes giving pipette resistances of 2.5 - 4.0 M Ω were used for recording. Following the conversion from 'cell-attached' to 'whole-cell' configuration, the cell/micropipette was left for ~30 seconds to allow the internal solution to equilibrate with the cell interior. Cell membrane potential was held at -50 mV before a voltage ramp from -120 mV to +80 mV was applied (20 mV increments). Measurements were taken with pClamp 10 software, through a Dell Inspiron computer, using an Axopatch 200B amplifier and a Digidata 1440 digitiser (all World Precision Instruments, UK).

Immunocytochemistry

HEK293 cells were harvested and fixed in 4% paraformaldehyde (Thermo Scientific). Cells were permeabilised in 0.01 M PBS with 0.1% Tween-20 and blocked in 5% donkey serum. Sections were incubated in mouse anti-human bestrophin-1 (1:250) for 1 hour at room temperature, washed in 0.01M PBS with 0.05% Tween-20 and then incubated in donkey anti-mouse IgG Alexa Fluor 488 (1:500) for 30 minutes at room temperature. See Supplementary Table 6 for antibody details. Cell nuclei were stained with Hoescht (diluted 1:10,000 with 0.01M PBS). Cells were imaged on a Leica LSM-700 confocal microscope with Zen software.

Graphical and Statistical Analysis

Graphpad Prism software was used to plot graphs and perform statistical analysis of all data. Data was analysed for normality using a Shapiro-Wilk test and then analysed with a one-way ANOVA (with Tukey's Multiple Comparisons test) or a Kruskal-Wallis test (with Dunn's Multiple Comparisons test) as appropriate.

Results

Confirmation of BEST1 expression

To confirm the identity of the protein expressed from the CAG.BEST1 transgene (Figure 1A), the immunoprecipitates resolved on a SDS-PAGE were analysed by Liquid Chromatography Tandem Mass Spectrometry (LC-MS/MS), achieving 62.4 % amino acid coverage (Figure 1B). The protein sequencing, combined with band size detection by western blot (Figure 1C) indicated that the protein was correctly translated from the CAG.BEST1 constructs.

Levels of BEST1 protein in HEK293 cells showed a four-fold increase when transduced with AAV.CAG.BEST1.WPRE compared to AAV.CAG.BEST1 vector (Figure 2). Both vectors were subsequently used to assess changes in chloride conductance *in vitro* with the expectation that cells transduced with the optimised vector containing WPRE would generate greater chloride conductance due to the enhanced levels of BEST1.

Increased chloride conductance *in vitro* following treatment with AAV.BEST1

Differences in current at +80 mV were statistically significant between AAV.CAG.BEST1 and un-transduced controls (n=10, p<0.05), but were not significantly different at +20, +40 and +60 mV. In contrast, chloride conductance was significantly higher at all voltage steps (+20, +40, +60 and +80 mV) between AAV.CAG.BEST1.WPRE (n=10) and un-transduced controls (n=10, p<0.001). There were no significant differences between the current values recorded from cells transduced with AAV.CAG.GFP.WPRE and un-transduced controls (figure 3A).

Equilibrium potential (reversal potential) for the buffers used in these experiments was calculated using the Nernst equation and was estimated at -33 mV. The reversal potential for cells averaged -13 mV for cells transduced with AAV.CAG.BEST1 and -20.3 mV for cells transduced with AAV.CAG.BEST1.WPRE.

Outward chord conductance (the gradient of the line of best fit of the I/V plots) are shown in Figure 3C. Differences were found to be statistically significant between un-transduced controls and both AAV.CAG.BEST1 (p<0.05) and AAV.CAG.BEST1.WPRE (p<0.001). Chord

conductance was 1.6-fold greater in HEK293 cells transduced with AAV.CAG.BEST1.WPRE compared to AAV.CAG.BEST1 ($p < 0.05$). There was no significant difference in conductance between un-transduced controls and cells transduced with AAV.CAG.GFP.WPRE. Taken together, the *in vitro* data indicate AAV2 delivery of *BEST1* to HEK293 cells generates increased levels of functional bestrophin-1 that significantly increases the chloride conductance of transduced cells, an effect that is enhanced by increased levels of BEST1.

To confirm the current was due to chloride conductance, the external chloride concentration was reduced from 147 mM to 7mM (achieved by replacing NaCl with sodium gluconate ($\text{NaC}_6\text{H}_{11}\text{O}_7$)). This resulted in significantly reduced current amplitudes in HEK293 cells transduced with AAV.CAG.BEST1.WPRE (Figure 4A). There were no significant differences between the current amplitudes of control HEK293 cells transduced with AAV.CAG.GFP.WPRE patched in either external solution.

Outward chord conductance was also significantly different between HEK293 cells transduced with AAV.CAG.BEST1.WPRE and controls, both in the high Cl^- and the low Cl^- external solution. No significant difference was seen between the high Cl^- and the low Cl^- external solution for HEK293 cells transduced with AAV.CAG.GFP.WPRE (Figure 4C).

Discussion

Autosomal recessive bestrophinopathy is a retinal degeneration for which there is currently no treatment. In recent years, gene therapy has emerged as a promising therapeutic strategy for similar conditions. Recent clinical trials in choroideremia and Leber congenital amaurosis (LCA) have produced promising results [17, 18, 26], resulting in FDA approval of the latter. Gene replacement therapy in choroideremia patients using an AAV vector, delivered by subretinal injection, have resulted in sustained increases in visual acuity up to 5 years post-treatment [27]. Pre-clinical demonstration of AAV gene therapy has also shown efficacy for X-linked RP caused by mutations in RPGR and clinical trials are ongoing [28, 29].

The recessive nature of ARB, as well as the relatively small size of the *BEST1* transgene, makes this condition an attractive target for AAV-mediated gene therapy. The characteristic shallow exudative retinal detachment associated with ARB may make the

subretinal injection less invasive, with no need to manually detach the retina prior to injection. Additionally, numerous AAV serotypes exhibit good tropism for RPE cells (AAV1, 2, 4, 5, 7, 8 and 9) [30], in particular AAV2 and AAV4 which have been used to successfully transduce the RPE in clinical trials [18, 20, 26]. Given that a recent study has shown a rescue effect in the canine model of ARB using an AAV strategy (23), a clinical trial using AAV.BEST1 vectors may be imminent. A critical feature of any AAV clinical trial is the ability to confirm the vector provides the therapeutic protein, and subsequent function, desired. To this end, we have developed an *in vitro* assay using HEK293 cells that enables quantification of increased chloride conductance that correlates to presence of BEST1 following transduction with AAV.BEST1 vectors. This provides a novel *in vitro* potency assay for future retinal gene therapy trials and introduces a technical innovation compared to other BEST1 gene therapy studies, where the bestrophin protein function (i.e. chloride conductance) was not measured [24, 25]. HEK293 cells are ideal for this purpose as they are electrophysiologically well characterized, are widely available and, unlike iPS-derived RPE or primary RPE cultures, can be easily standardized to GMP level for clinical testing. As such whole-cell patch-clamp in HEK293 cells provides a robust, reproducible and highly sensitive assay for the testing of AAV-mediated BEST1 transfer. Such assays are important for testing equivalency between vector batches and for confirming vector efficacy prior to administration to patients.

We also demonstrated increases in Bestrophin-1 protein levels and chloride conductance following the use inclusion of a WPRE in the vector construct. This increase in chloride conductance could allow a lower dose of AAV to be administered to patients, reducing the likelihood of potential immune responses. However it could also lead to a toxic effect in the retina if the expression is not limited to the RPE and *in vivo* studies will be required to confirm this.

In summary, BEST1 AAV gene therapy vectors are showing encouraging signs of being appropriate for translation to the clinic. Here we have built on the current body of work assessing such vectors and have shown for the first time successful development of a functional assay for the assessment of BEST1 protein following AAV delivery. This

development will be critical if gene therapy treatments for bestrophinopathies are to move into clinical trial.

Acknowledgements

We would like to thank Fight for Sight UK for funding this work. We would also like to thank Monika Stegmann from the Department of Biochemistry at the University of Oxford for her help with the proteomic analysis.

Disclosure Statement

Robert MacLaren receives funding from Nightstar Therapeutics and Fight for Sight for research into Best disease gene therapy, the other authors have no conflicts of interest to declare.

References

1. Boon, C.J., et al., *The spectrum of ocular phenotypes caused by mutations in the BEST1 gene*. Prog Retin Eye Res, 2009. **28**(3): p. 187-205.
2. Burgess, R., et al., *Biallelic mutation of BEST1 causes a distinct retinopathy in humans*. American Journal of Human Genetics, 2008. **82**(1): p. 19-31.
3. Boon, C.J., et al., *Autosomal recessive bestrophinopathy: differential diagnosis and treatment options*. Ophthalmology, 2013. **120**(4): p. 809-20.
4. Johnson, A.A., et al., *Bestrophin 1 and retinal disease*. Prog Retin Eye Res, 2017.
5. Marmorstein, A.D., et al., *Bestrophin, the product of the Best vitelliform macular dystrophy gene (VMD2), localizes to the basolateral plasma membrane of the retinal pigment epithelium*. Proc Natl Acad Sci U S A, 2000. **97**(23): p. 12758-63.
6. Hartzell, H.C., et al., *Molecular physiology of bestrophins: multifunctional membrane proteins linked to best disease and other retinopathies*. Physiol Rev, 2008. **88**(2): p. 639-72.
7. Guziewicz, K.E., et al., *Bestrophinopathy: An RPE-photoreceptor interface disease*. Prog Retin Eye Res, 2017. **58**: p. 70-88.
8. Milenkovic, A., et al., *Bestrophin 1 is indispensable for volume regulation in human retinal pigment epithelium cells*. Proc Natl Acad Sci U S A, 2015. **112**(20): p. E2630-9.
9. Vaisey, G., A.N. Miller, and S.B. Long, *Distinct regions that control ion selectivity and calcium-dependent activation in the bestrophin ion channel*. Proc Natl Acad Sci U S A, 2016. **113**(47): p. E7399-E7408.
10. Zhang, Y., et al., *ATP activates bestrophin ion channels through direct interaction*. Nat Commun, 2018. **9**(1): p. 3126.
11. Sun, H., et al., *The vitelliform macular dystrophy protein defines a new family of chloride channels*. Proceedings of the National Academy of Sciences of the United States of America, 2002. **99**(6): p. 4008-4013.
12. Kane Dickson, V., L. Pedi, and S.B. Long, *Structure and insights into the function of a Ca(2+)-activated Cl(-) channel*. Nature, 2014. **516**(7530): p. 213-8.

13. Kane Dickson, V., *Phasing and structure of bestrophin-1: a case study in the use of heavy-atom cluster compounds with multi-subunit transmembrane proteins*. Acta Crystallogr D Struct Biol, 2016. **72**(Pt 3): p. 319-25.
14. Davidson, A.E., et al., *Functional Characterization of Bestrophin-1 Missense Mutations Associated with Autosomal Recessive Bestrophinopathy*. Investigative Ophthalmology & Visual Science, 2011. **52**(6): p. 3730-3736.
15. Guziewicz, K.E., et al., *Bestrophin gene mutations cause canine multifocal retinopathy: a novel animal model for best disease*. Invest Ophthalmol Vis Sci, 2007. **48**(5): p. 1959-67.
16. Marmorstein, L.Y., et al., *The light peak of the electroretinogram is dependent on voltage-gated calcium channels and antagonized by bestrophin (best-1)*. J Gen Physiol, 2006. **127**(5): p. 577-89.
17. Bainbridge, J.W., et al., *Long-term effect of gene therapy on Leber's congenital amaurosis*. N Engl J Med, 2015. **372**(20): p. 1887-97.
18. Maclaren, R.E., et al., *Retinal gene therapy in patients with choroideremia: initial findings from a phase 1/2 clinical trial*. Lancet, 2014.
19. Edwards, T.L., et al., *Visual Acuity after Retinal Gene Therapy for Choroideremia*. N Engl J Med, 2016. **374**(20): p. 1996-8.
20. Ghazi, N.G., et al., *Treatment of retinitis pigmentosa due to MERTK mutations by ocular subretinal injection of adeno-associated virus gene vector: results of a phase I trial*. Hum Genet, 2016. **135**(3): p. 327-43.
21. Auricchio, A. and F. Rolling, *Adeno-associated viral vectors for retinal gene transfer and treatment of retinal diseases*. Curr Gene Ther, 2005. **5**(3): p. 339-48.
22. Surace, E.M. and A. Auricchio, *Adeno-associated viral vectors for retinal gene transfer*. Prog Retin Eye Res, 2003. **22**(6): p. 705-19.
23. Surace, E.M. and A. Auricchio, *Versatility of AAV vectors for retinal gene transfer*. Vision Res, 2008. **48**(3): p. 353-9.
24. Guziewicz, K.E., et al., *Recombinant AAV-mediated BEST1 transfer to the retinal pigment epithelium: analysis of serotype-dependent retinal effects*. PLoS One, 2013. **8**(10): p. e75666.

25. Guziewicz, K.E., et al., *BEST1 gene therapy corrects a diffuse retina-wide microdetachment modulated by light exposure*. Proc Natl Acad Sci U S A, 2018.
26. Weleber, R.G., et al., *Results at 2 Years after Gene Therapy for RPE65-Deficient Leber Congenital Amaurosis and Severe Early-Childhood-Onset Retinal Dystrophy*. Ophthalmology, 2016. **123**(7): p. 1606-20.
27. Xue, K., et al., *Beneficial effects on vision in patients undergoing retinal gene therapy for choroideremia*. Nat Med, 2018. **24**(10): p. 1507-1512.
28. Fischer, M.D., et al., *Codon-Optimized RPGR Improves Stability and Efficacy of AAV8 Gene Therapy in Two Mouse Models of X-Linked Retinitis Pigmentosa*. Mol Ther, 2017. **25**(8): p. 1854-1865.
29. Beltran, W.A., et al., *Optimization of Retinal Gene Therapy for X-Linked Retinitis Pigmentosa Due to RPGR Mutations*. Mol Ther, 2017. **25**(8): p. 1866-1880.
30. Castle, M.J., et al., *Controlling AAV Tropism in the Nervous System with Natural and Engineered Capsids*. Methods Mol Biol, 2016. **1382**: p. 133-49.

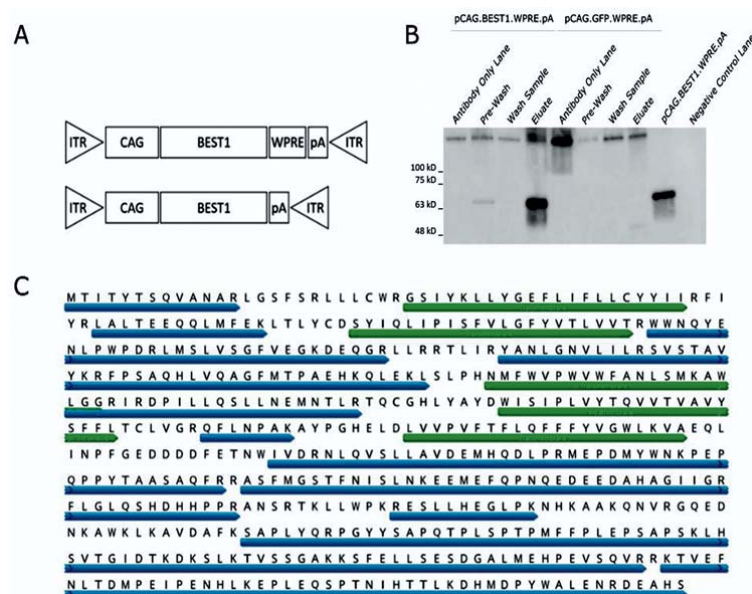


Figure 1. Vector design and BEST1 protein sequence. (A) Schematic representation of rAAV.BEST1 vectors used in this study. The common features to both expression cassettes are the cytomegalovirus early enhancer and chicken β -actin hybrid promoter (CAG); the coding sequence for BEST1 protein (BEST1) and the polyadenylation signal from the bovine growth hormone (pA), all flanked by the AAV2 inverted terminal repeats (ITR). Additionally, one of the plasmids contain the Woodchuck hepatitis virus posttranscriptional regulatory element (WPRE) downstream the coding sequence. (B) Successful immunoprecipitation of human Bestrophin-1 from HEK293 lysates transfected with CAG.BEST1 plasmids, was confirmed by western blotting, using a mouse anti-human Bestrophin-1 antibody. Bands are seen at ~67 kD in BEST1-transfected eluates and control sample that are not present in wash samples and GFP-transfected controls. (C) Bestrophin-1 sequence was confirmed by liquid chromatography-tandem mass spectrometry (LC-MS/MS). 362 amino acids, mainly in the C-terminal regional, were covered following this approach (blue arrows below the amino acid sequence). The low coverage achieved in the N-terminus could be explained by the presence of transmembrane domains in that region where cleavage sites are less frequent or absent (green arrows below the amino acid sequence).

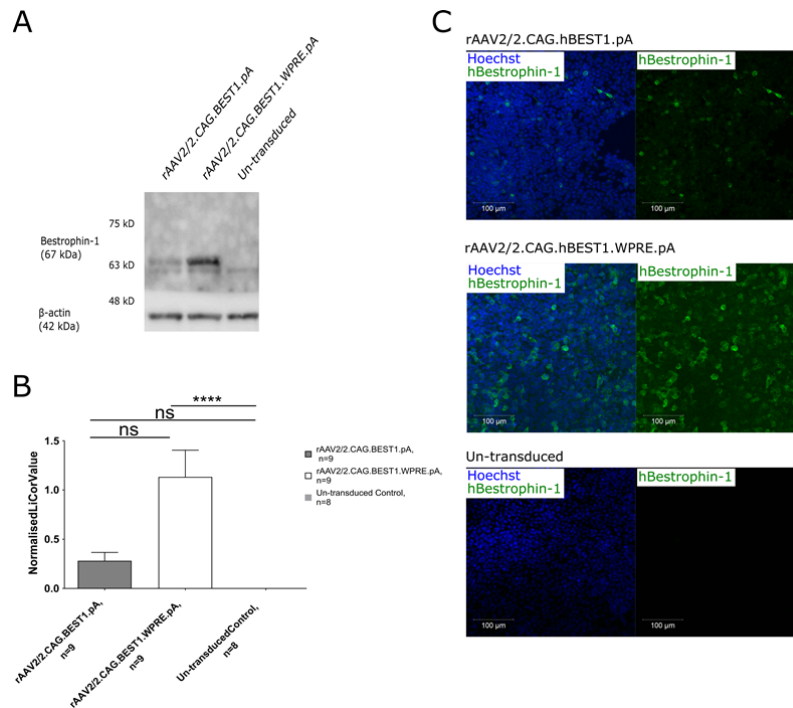


Figure 2. Expression of bestrophin-1 in HEK293 cells following transduction with rAAV2/2-BEST1 vectors. (A) Representative western blot shows bestrophin-1 expression in HEK293 cells following transduction. Bands migrating at the expected size (~67 kD) indicate the presence of human bestrophin-1 in the transduced cells and its absence from the un-transduced control cells. (B) Quantification of bestrophin-1 expression using pixel density from western blot bands, human bestrophin-1 was normalized to β -actin. (C) Bestrophin-1 expression is seen in cells transduced with rAAV2/2-BEST1 vectors and is absent in the un-transduced cells. Error bars = SEM. **** = $p < 0.0001$ by Kruskal-Wallis test with Dunn's test for multiple comparisons.

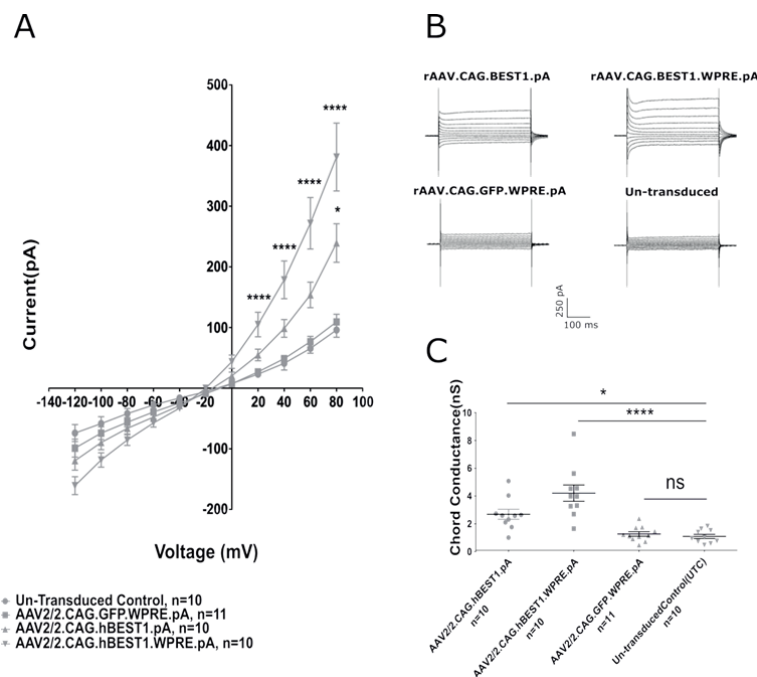


Figure 3. Whole-cell patch-clamp of HEK293 cells transduced with rAAV2/2-BEST1 vectors. (A) Current/Voltage (I/V) plots for HEK293 cells transduced with rAAV2/2-BEST1 vectors and controls. Current values at +20 mV, +40 mV, +60 mV and +80 mV were analysed via a one-way ANOVA and significance was defined as $p < 0.05$. HEK293 with either rAAV2/2.CAG.BEST1.pA ($n=10$) or rAAV2/2.CAG.BEST1.WPRE.pA ($n=10$) vectors show increased current amplitude over control cells transduced with rAAV2/2.CAG.GFP.WPRE.pA ($n=11$) or left untransduced. There was a significant increase in current amplitude in cells transduced with rAAV2/2.CAG.BEST1.WPRE.pA compared to rAAV2/2.CAG.BEST1.pA. There was no significant change in chloride conductance in rAAV2/2.CAG.GFP.WPRE.pA-transduced HEK293 cells and un-transduced controls. (B) Current waveforms for each experimental group. (C) Outward chord conductance for HEK293 cells transduced with rAAV2/2-BEST1 vectors and controls. Significant differences were found between HEK293 cells transduced with either rAAV2/2.CAG.BEST1.pA or rAAV2/2.CAG.BEST1.WPRE.pA compared to untransduced cells via one-way ANOVA ($p < 0.05$). There was no significant difference between rAAV2/2.CAG.GFP.WPRE.pA-transduced cells and untransduced controls. Error bars = SEM. * = $p < 0.05$, **** = $p < 0.0001$ by one-way ANOVA with Tukey's multiple comparisons.

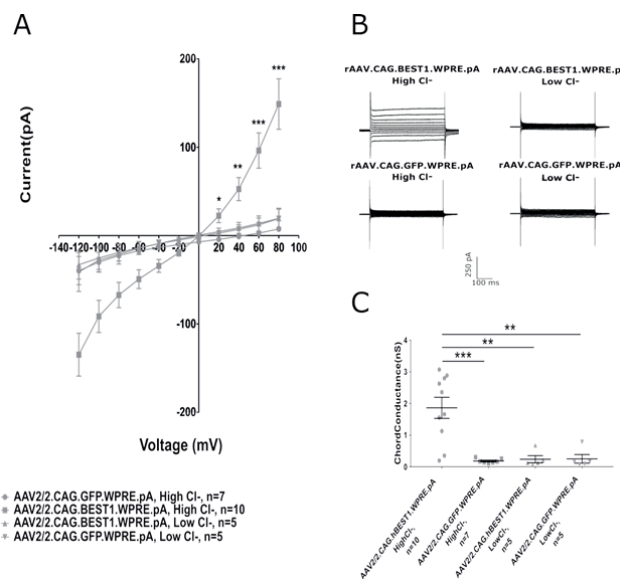


Figure 4. Whole-cell patch-clamp of HEK293 cells transduced with rAAV2/2.CAG.BEST1.WPRE.pA vectors in high and low Cl⁻ buffers. (A) Current/Voltage (I/V) plots for HEK293 cells transduced with rAAV2/2.CAG.BEST1.WPRE.pA and controls. Current values at +20 mV, +40 mV, +60 mV and +80 mV were analysed via a Kruskal-Wallis test and significance was defined as $p < 0.05$. HEK293 transduced with rAAV2/2.CAG.BEST1.WPRE.pA ($n=10$) show increased current amplitude over control cells transduced with rAAV2/2.CAG.GFP.WPRE.pA ($n=7$) in the high Cl⁻ buffer. There was a significant decrease in current amplitude in cells transduced with rAAV2/2.CAG.BEST1.WPRE.pA patched in low Cl⁻ buffer ($n=5$) compared to those in the high Cl⁻ buffer. There was no significant change in current amplitude in rAAV2/2.CAG.GFP.WPRE.pA-transduced HEK293 cells patched in high or low Cl⁻ buffer. **(B)** Current waveforms for each experimental group. **(C)** Outward chord conductance for HEK293 cells transduced with rAAV2/2.CAG.BEST1.WPRE.pA and controls. Data was analysed using a Kruskal-Wallis test and significance was defined as $p < 0.05$. Significant decreases in conductance were seen in HEK293 cells, transduced with rAAV2/2.CAG.BEST1.WPRE.pA, in the low Cl⁻ buffer compared to the high Cl⁻ buffer. There was no significant difference between rAAV2/2.CAG.GFP.WPRE.pA-transduced cells patched in high or low Cl⁻ buffer. Error bars = SEM. * = $p < 0.05$, **** = $p < 0.0001$ by Kruskal-Wallis test with Dunn's test for multiple comparisons.

Supplementary Table 1. Shapiro-Wilk Test for Normality for bestrophin-1 expression levels in HEK293 cells transduced with AAV-BEST1 vectors.

Shapiro-Wilk normality test	AAV2/2.CAG.hBEST1.pA	AAV2/2.CAG.hBEST1.WPRE.pA	Un-transduced Control
N Number	9	9	8
W	0.9238	0.8228	0.9761
P value	0.4247	0.0371	0.941
Passed normality test (alpha=0.05)?	Yes	No	Yes
P value summary	ns	*	ns

Supplementary Table 2. Shapiro-Wilk Test for Normality for current amplitudes in HEK293 cells transduced with AAV-BEST1 vectors.

Shapiro-Wilk normality test	AAV2/2.CAG.hBEST1.pA	AAV2/2.CAG.hBEST1.WPRE.pA	AAV2/2.CAG.GFP.WPRE.pA	Un-transduced Control (UTC)
N Number	10	10	11	10
20 mV				
W	0.9073	0.9651	0.966	0.982
P value	0.3352	0.8573	0.8434	0.9749
Passed normality test (alpha=0.05)?	Yes	Yes	Yes	Yes
P value summary	ns	ns	ns	ns
40 mV				
W	0.9006	0.9594	0.9457	0.9658
P value	0.2924	0.8041	0.5901	0.849
Passed normality test (alpha=0.05)?	Yes	Yes	Yes	Yes
P value summary	ns	ns	ns	ns
60 mV				
W	0.8675	0.8535	0.9596	0.9591
P value	0.0934	0.064	0.7669	0.7752
Passed normality test (alpha=0.05)?	Yes	Yes	Yes	Yes
P value summary	ns	ns	ns	ns
80 mV				
W	0.908	0.8879	0.9653	0.9515
P value	0.2677	0.1604	0.8358	0.6857
Passed normality test (alpha=0.05)?	Yes	Yes	Yes	Yes
P value summary	ns	ns	ns	ns

This paper has been peer-reviewed and accepted for publication, but has yet to undergo copyediting and proof correction. The final published version may differ from this proof.

Supplementary Table 3. Shapiro-Wilk Test for Normality for chord conductance in HEK293 cells transduced with AAV-BEST1 vectors.

Shapiro-Wilk normality test	AAV2/2.CAG.hBEST1.pA	AAV2/2.CAG.hBEST1.WPRE.pA	AAV2/2.CAG.GFP.WPRE.pA	Un-transduced Control (UTC)
N Number	10	10	11	10
Chord Conductance				
W	0.9062	0.9065	0.9633	0.9325
P value	0.2557	0.2575	0.812	0.4724
Passed normality test (alpha=0.05)?	Yes	Yes	Yes	Yes
P value summary	ns	ns	ns	ns

Supplementary Table 4. Shapiro-Wilk Test for Normality for current amplitude in Cl⁻ reduction experiments.

Shapiro-Wilk normality test	AAV2/2.CAG.BEST1.WPRE High Cl ⁻	AAV2/2.CAG.GFP.WPRE High Cl ⁻	AAV2/2.CAG.BEST1.WPRE Low Cl ⁻	AAV2/2.CAG.GFP.WPRE Low Cl ⁻
N Number	10	7	5	5
20 mV				
W	0.876	0.9014	0.6439	0.6533
P value	0.2094	0.227	0.0023	0.0029
Passed normality test (alpha=0.05)?	Yes	Yes	No	No
P value summary	ns	ns	**	**
40 mV				
W	0.9305	0.9634	0.6476	0.6094
P value	0.4524	0.847	0.0025	0.0008
Passed normality test (alpha=0.05)?	Yes	Yes	No	No
P value summary	ns	ns	**	***
60 mV				
W	0.9201	0.9596	0.6489	0.632
P value	0.358	0.8156	0.0026	0.0016
Passed normality test (alpha=0.05)?	Yes	Yes	No	No
P value summary	ns	ns	**	**
80 mV				
W	0.959	0.9247	0.7133	0.6473
P value	0.8103	0.3981	0.0131	0.0025
Passed normality test (alpha=0.05)?	Yes	Yes	No	No
P value summary	ns	ns	*	**

Shapiro-Wilk normality test	AAV2/2.CAG.BEST1.WPRE High Cl-	AAV2/2.CAG.GFP.WPRE High Cl-	AAV2/2.CAG.BEST1.WPRE Low Cl-	AAV2/2.CAG.GFP.WPRE Low Cl-
N Number	10	7	5	5
W	0.9052	0.8722	0.7273	0.6668
P value	0.2494	0.194	0.0181	0.0042
Passed normality test (alpha=0.05)?	Yes	Yes	No	No
P value summary	ns	ns	*	**

Supplementary Table 6. Table of antibodies.

Target	Species Raised In	Supplier	Catalogue Number
Human Bestrophin-1	Mouse	Abcam	ab2182
β -actin	Rabbit	Abcam	ab8227
Mouse IgG	Donkey	Abcam	ab98799